## Supplementary Figures

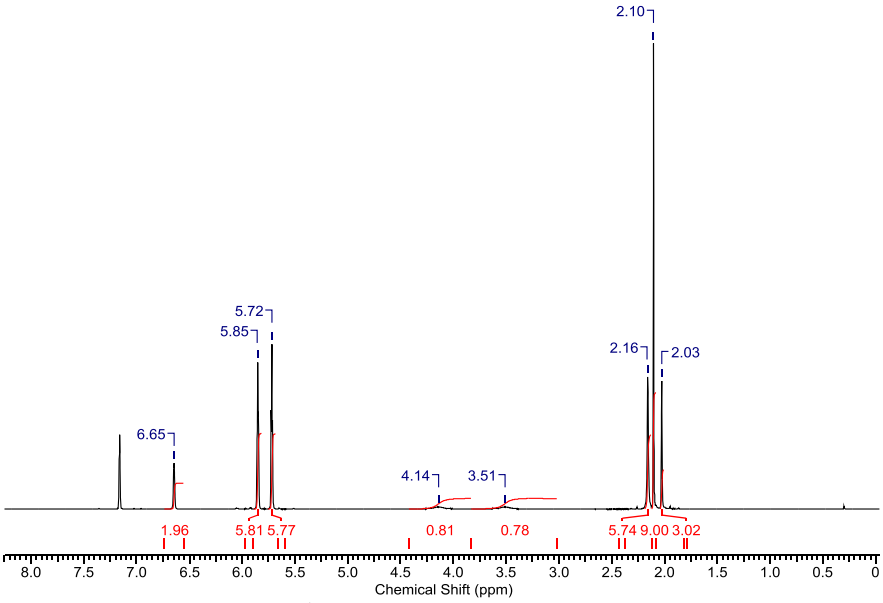


**Supplementary Figure 1.** $^{1}$H NMR spectrum of **1-Y** in benzene-$D_6$ at 298 K.

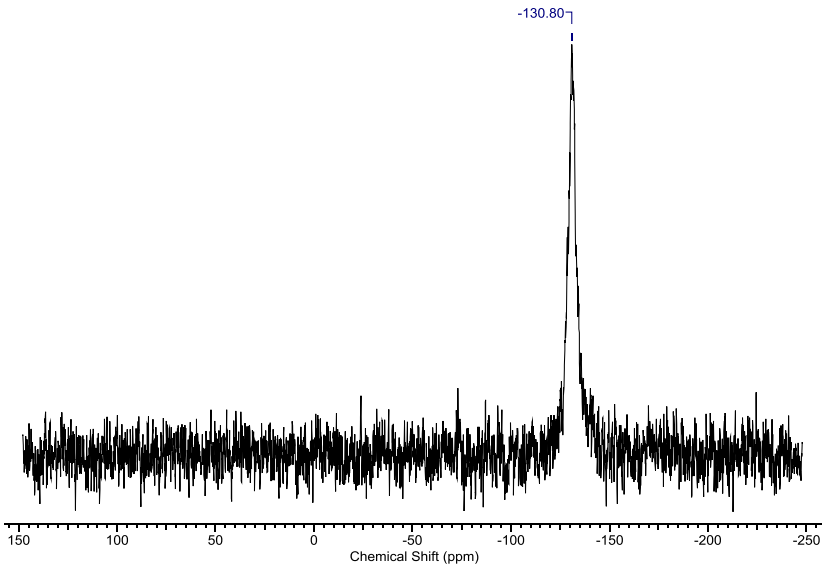


**Supplementary Figure 2.** $^{31}$P NMR spectrum of **1-Y** in benzene-$D_6$ at 298 K.

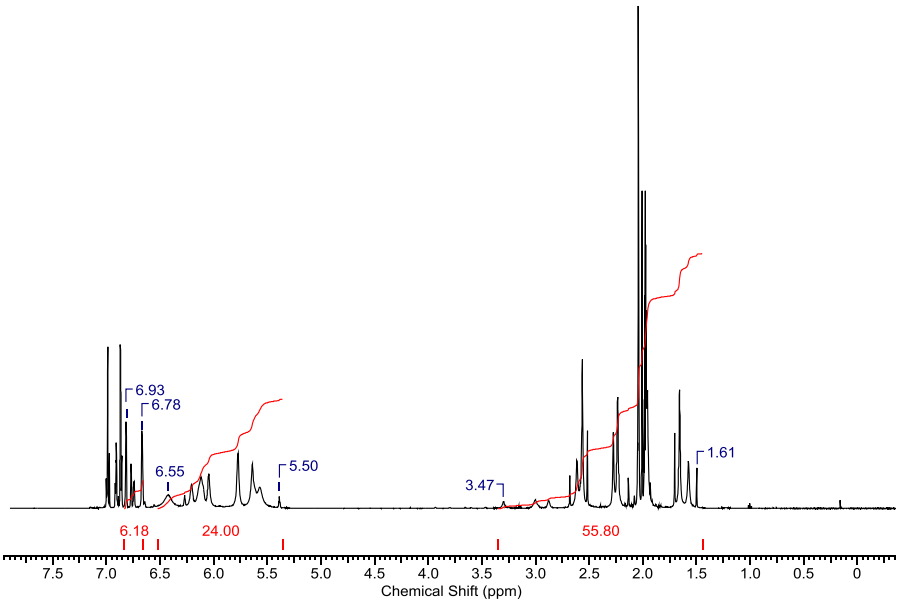


**Supplementary Figure 3.** $^{1}$H NMR spectrum of **2-Y**·toluene in toluene-$D_8$ at 298 K. The integral for the region 1.61-3.47 ppm includes residual protons in the solvent, which overlap with the resonances due to **2-Y**.

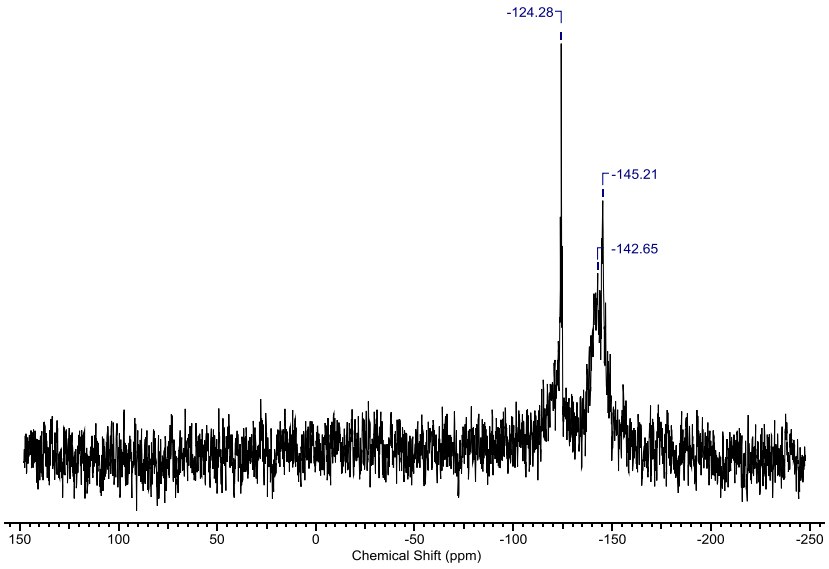


**Supplementary Figure 4.** $^{31}$P{$^{1}$H} NMR spectrum of **2-Y**·toluene in toluene-$D_8$ at 298 K.

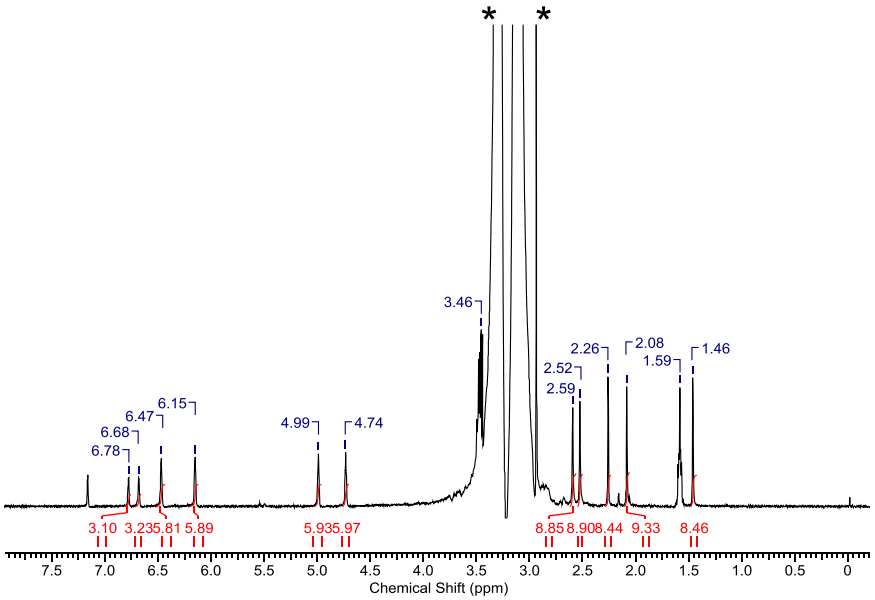


**Supplementary Figure 5.** $^{1}$H NMR spectrum of [**3-Y**][Li(thf)$_4$]$_2$·thf recorded in a mixture of dimethoxyethane ($C_4H_{10}O_2$) and two drops of benzene-$D_6$ at 298 K in thf-$D_8$ at 298 K.

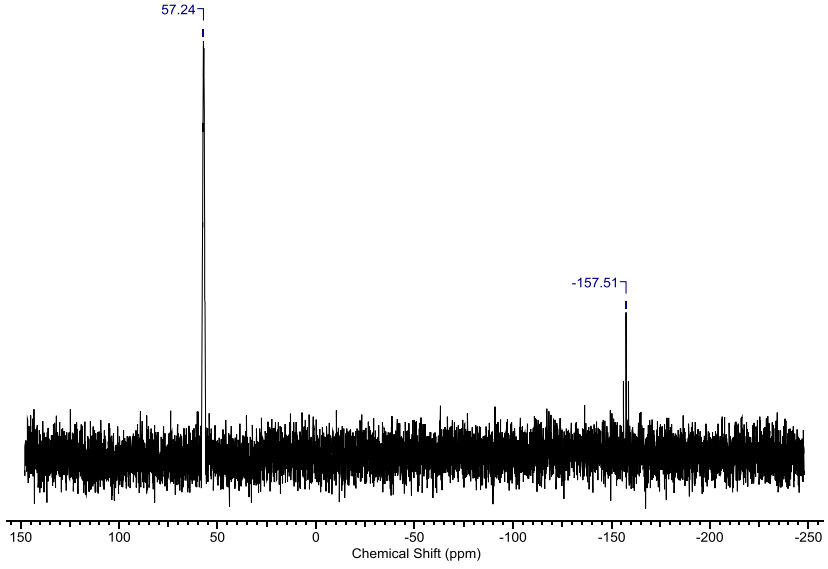


**Supplementary Figure 6.** $^{1}$H-coupled $^{31}$P NMR spectrum of [**3-Y**][Li(thf)$_4$]$_2$·thf recorded in a mixture of dimethoxyethane ($C_4H_{10}O_2$) and two drops of benzene-$D_6$ at 298 K in thf-$D_8$ at 298 K.

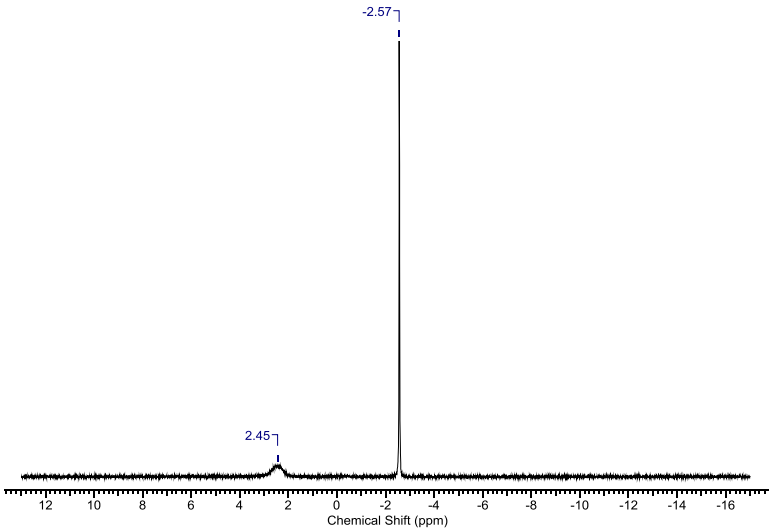


**Supplementary Figure 7.** $^{7}$Li NMR spectrum of [**3-Y**][Li(thf)$_4$]$_2$·thf recorded in a mixture of dimethoxyethane ($C_4H_{10}O_2$) and two drops of benzene-$D_6$ at 298 K in thf-$D_8$ at 298 K..

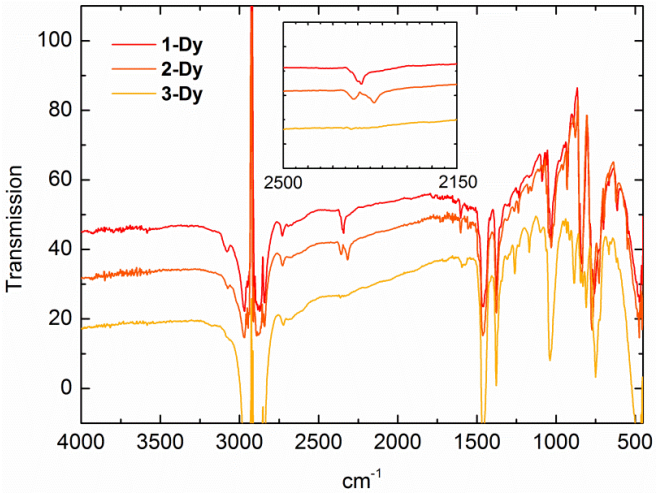


**Supplementary Figure 8**. Infrared spectra (Nujol mulls) of **1-Dy** ($\tilde{\nu}_{P-H}$ = 2342 cm$^{-1}$), **2-Dy**·toluene ($\tilde{\nu}_{P-H}$ = 2318, 2358 cm$^{-1}$) and [Li(thf)$_4$]$_2$[**3-Dy**]·thf.

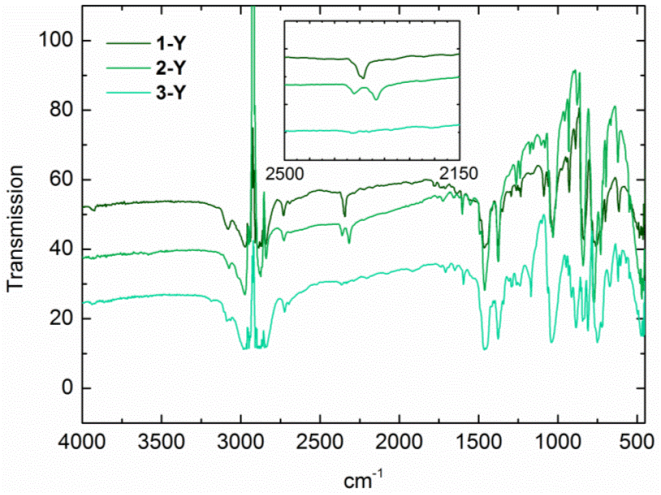


**Supplementary Figure 9**. Infrared spectra (Nujol mulls) of **1-Y** ($\tilde{\nu}_{P–H}$ = 2344 $cm^{-1}$), **2-Y**·toluene ($\tilde{\nu}_{P–H}$ = 2316, 2362 $cm^{-1}$) and $[Li(thf)_4]_2$[**3-Y**]·thf.

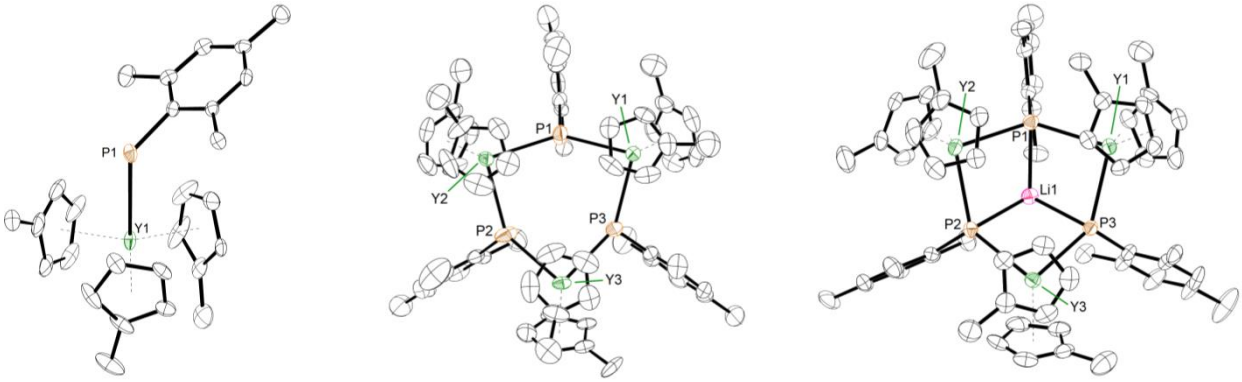


**Supplementary Figure 10.** Thermal ellipsoid representations (50% probability) of the molecular structures of **1-Y** (left), **2-Y** (centre) and **3-Y** (right). For clarity, hydrogens atoms are omitted from **1-Y** and **2-Y**.

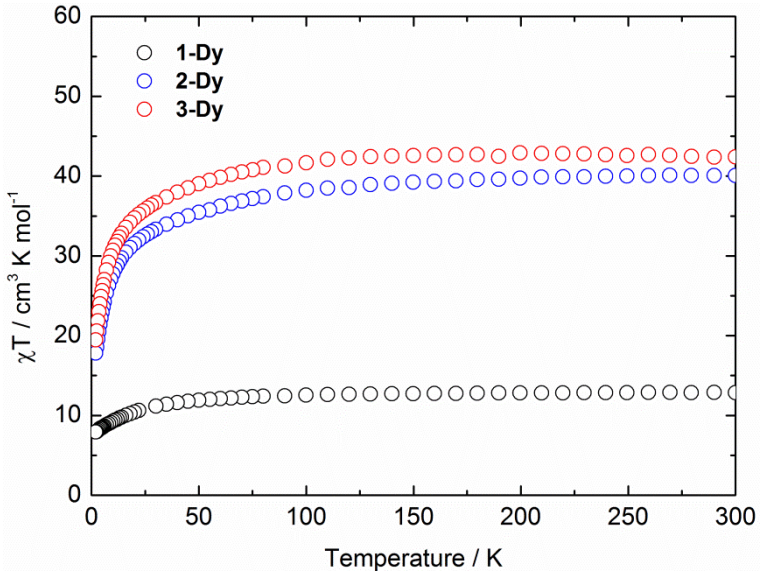


**Supplementary Figure 11.** Temperature dependence of the product of the molar magnetic susceptibility ($\chi_M$) with temperature for **1-Dy**, **2-Dy**·toluene, [**3-Dy**][Li(thf)$_4$]$_2$·thf.

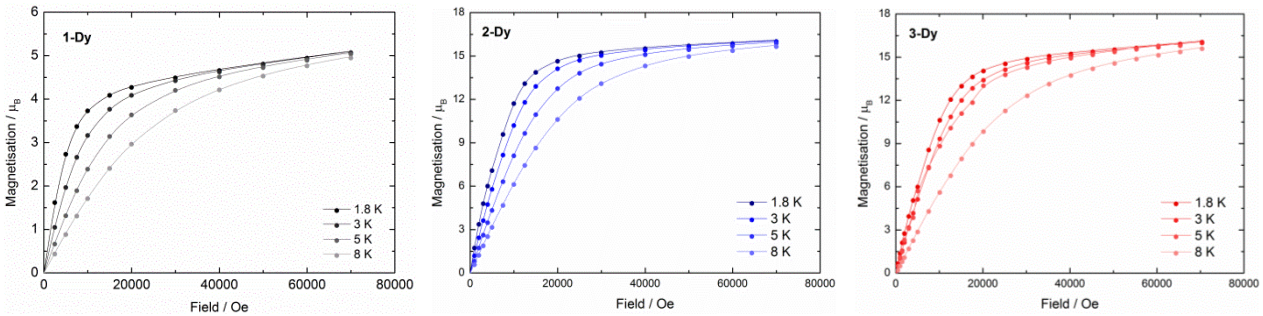


**Supplementary Figure 12.** Field dependence of the magnetization for **1-Dy** (left), **2-Dy**·toluene (centre) and [**3-Dy**][Li(thf)$_4$]$_2$·thf (right) at temperatures in the range 1.8-8 K.

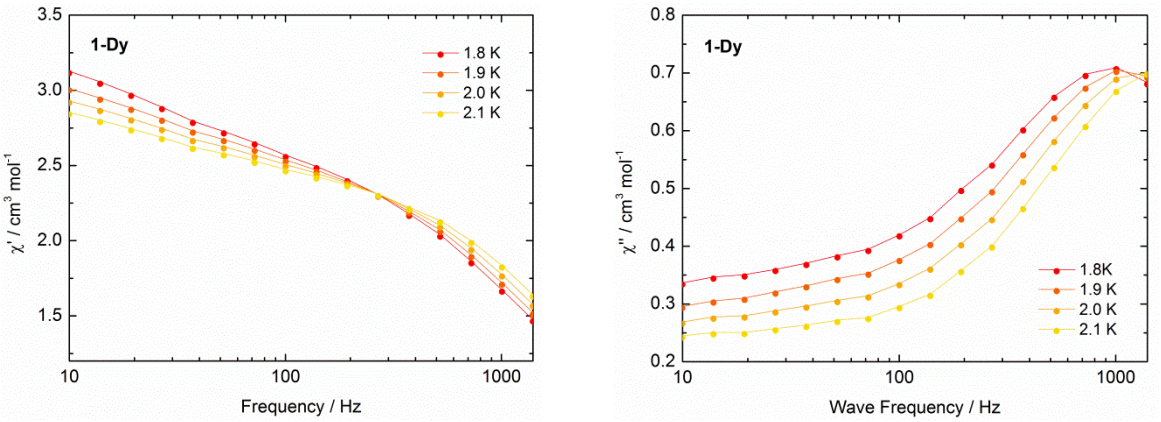


**Supplementary Figure 13.** Frequency dependence of the in-phase ($\chi'$) and the out-of-phase ($\chi''$) magnetic susceptibility for **1-Dy** using an oscillating field of $H_{ac}$ = 1.55 Oe and zero applied field.

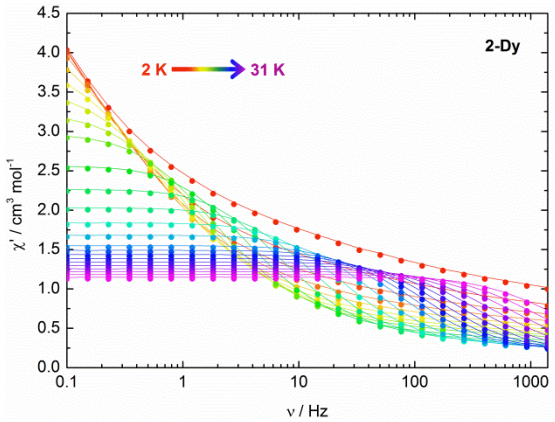


**Supplementary Figure 14.** Frequency dependence of the in-phase ($\chi'$) magnetic susceptibility for **2-Dy** using an oscillating field of $H_{ac}$ = 1.55 Oe and zero applied field.

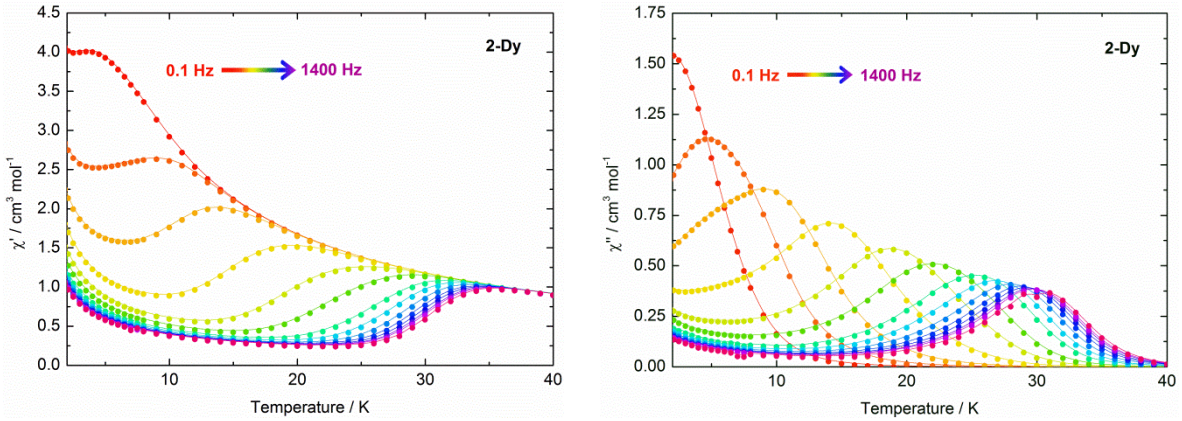


**Supplementary Figure 15.** Temperature dependence of the in-phase ($\chi'$) and the out-of-phase ($\chi''$) magnetic susceptibility for **2-Dy**, using an oscillating field of $H_{ac}$ = 1.55 Oe and zero applied field.

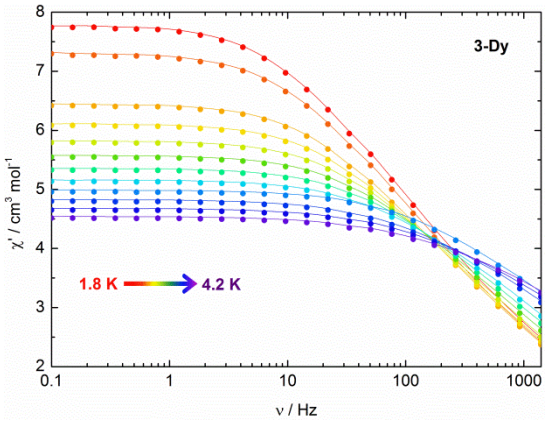


**Supplementary Figure 16.** Frequency dependence of the in-phase ($\chi'$) magnetic susceptibility for [**3-Dy**]$^-$, using an oscillating field of $H_{ac}$ = 1.55 Oe and zero applied field.

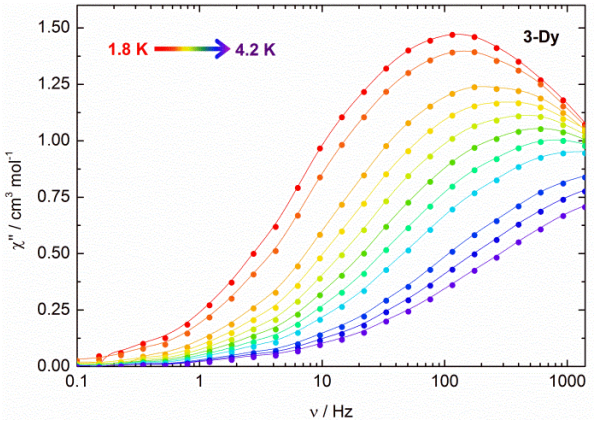


**Supplementary Figure 17.** Frequency dependence of the out-of-phase ($\chi''$) magnetic susceptibility for [**3-Dy**]$^-$, using an oscillating field of $H_{ac}$ = 1.55 Oe and zero applied field.

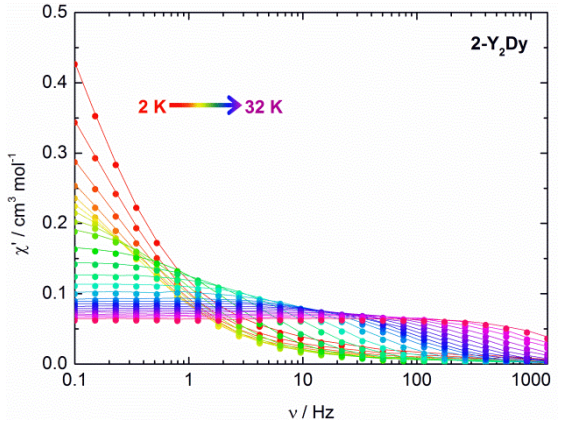


**Supplementary Figure 18.** Frequency dependence of the in-phase ($\chi'$)magnetic susceptibility for **2-Y$_2$Dy** in a matrix of **2-Y** (1:20 Dy:Y). Data collected using an oscillating field of $H_{ac}$ = 1.55 Oe and zero applied field.

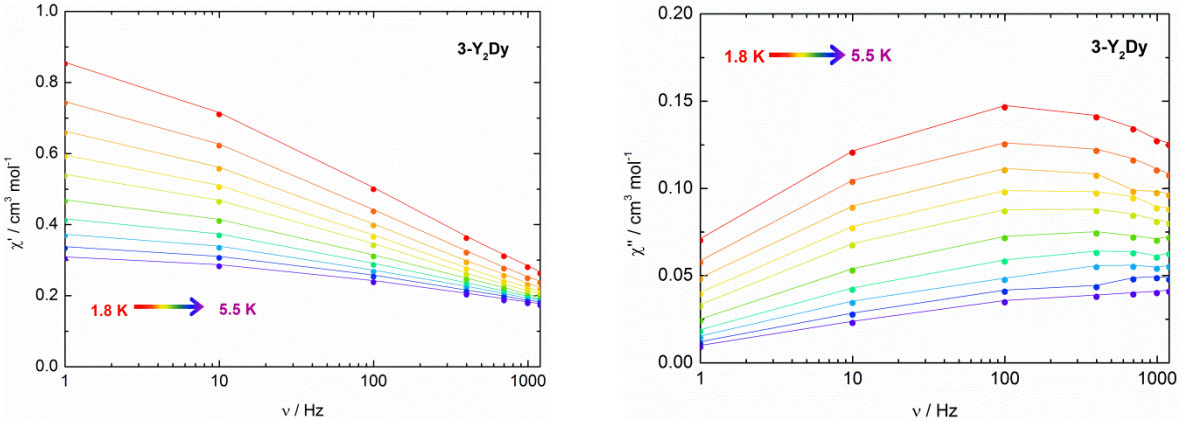


**Supplementary Figure 19.** Frequency dependence of the in-phase ($\chi'$) and the out-of-phase ($\chi''$) magnetic susceptibility for [**3-Y$_2$Dy**][Li(thf)$_4$]$_2$ in a matrix of [**3-Y**][Li(thf)$_4$]$_2$ (1:20 Dy:Y). Data collected using an oscillating field of $H_{ac}$ = 1.55 Oe and zero applied field.

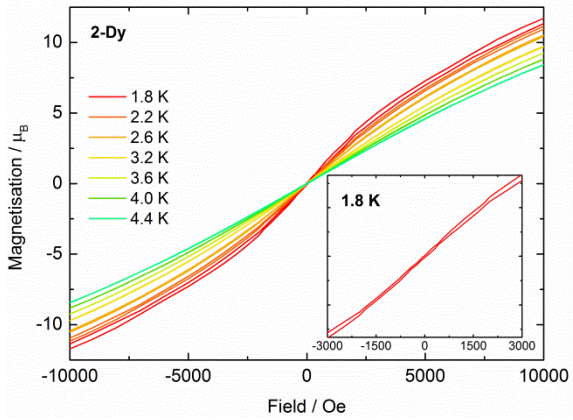


**Supplementary Figure 20.** Field ($H$) dependence of the magnetization ($M$) for undiluted **2-Dy** at $T$ = 1.8 K with $H$ = ±5 T. Inset: expansion of the region with $H$ = ±3000 Oe showing the small opening of the hysteresis loop.

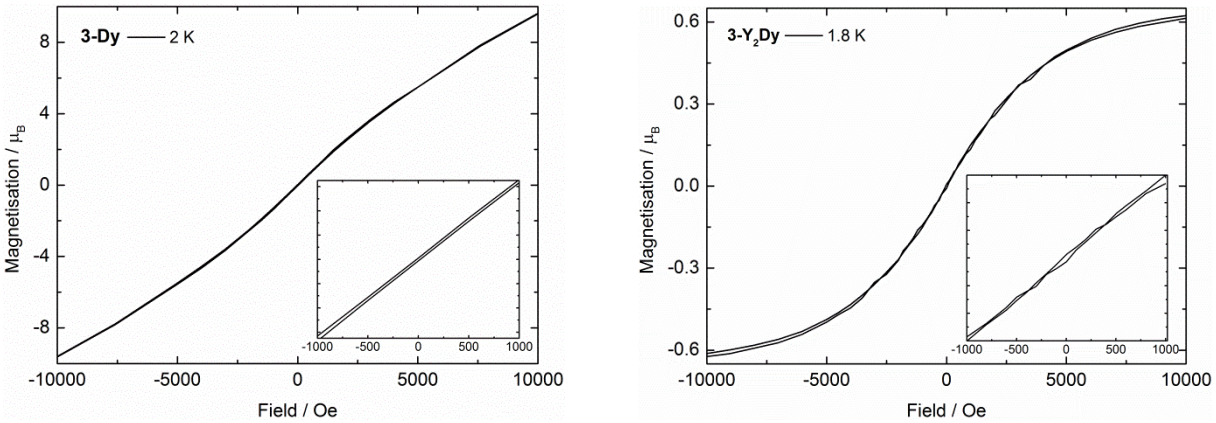


**Supplementary Figure 21.** Field (*H*) dependence of the magnetization (*M*) for undiluted **3-Dy** (left) and diluted **3-$Y_2$Dy** (right) at *T* = 1.8 K and 2 K, respectively, with *H* = ±5 T. Inset: expansion of the region with *H* = ±1000 Oe showing the small opening of the hysteresis loop.

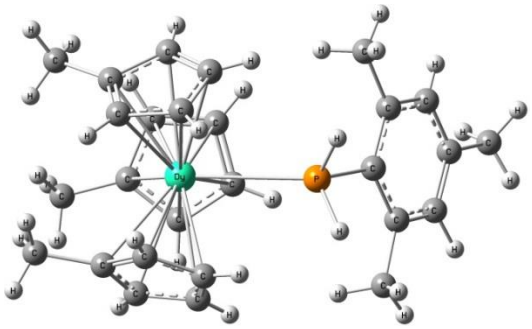

**Supplementary Figure 22.** Calculated structure of **1-Dy**.

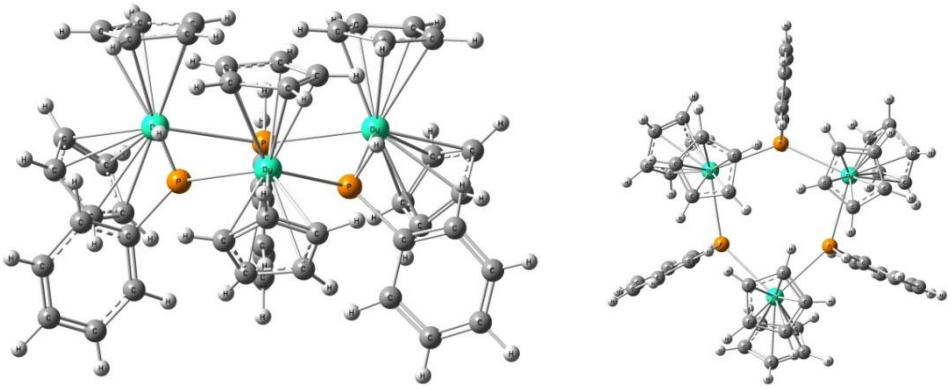

**Supplementary Figure 23.** Calculated structure of **2-Dy**.

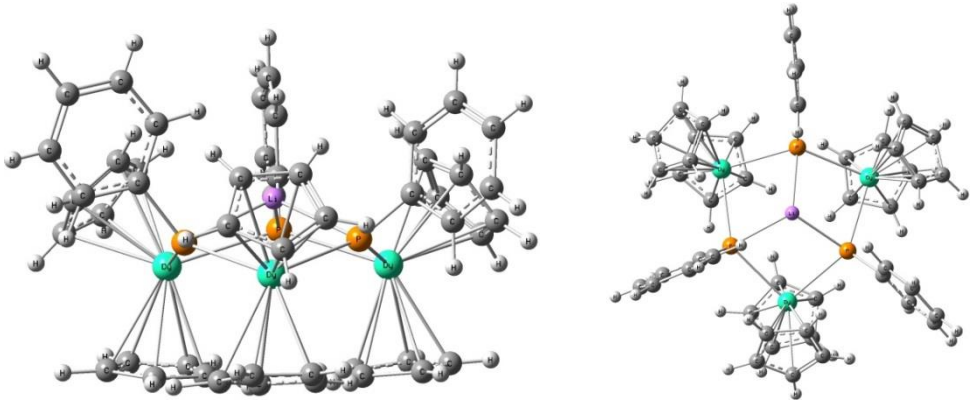

**Supplementary Figure 24.** Calculated structure of **3-Dy**.

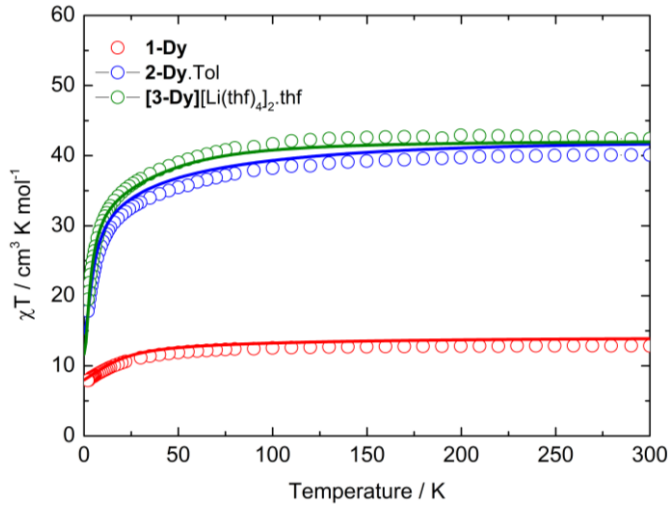


**Supplementary Figure 25.** Calculated temperature dependence of the product of the molar magnetic susceptibility ($\chi_M$) with temperature (solid lines) for **1-Dy**, **2-Dy**·toluene, [**3-Dy**][Li(thf)$_4$]$_2$·thf compared to the experimental data (circles).

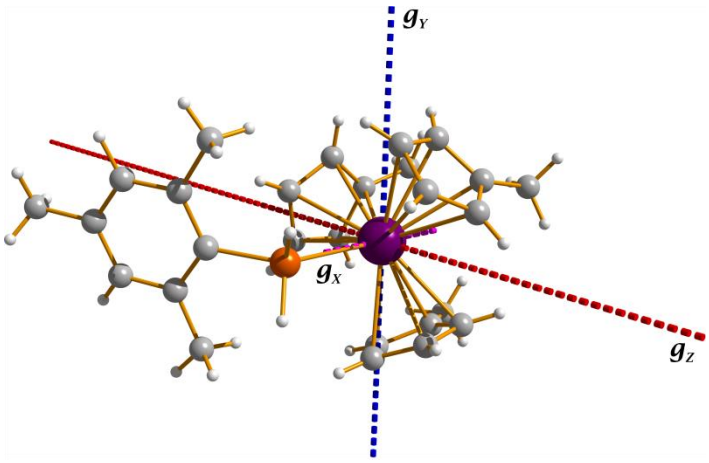


**Supplementary Figure 26.** Orientation of the magnetic axes in the ground Kramers' doublets for **1-Dy**. The Dy–P bond and the $g_z$ axis create an angle of 88.4°.

## Supplementary Tables

**Supplementary Table 1.** Crystal data and structure refinement details. MoKα (λ = 0.71073)

| | **1-Dy** | **2-Dy·toluene** | **[3-Dy][Li(thf)$_4$]$_2$·thf** | **1-Y** | **2-Y·toluene** | **[3-Y][Li(thf)$_4$]$_2$·thf** |
|---|---|---|---|---|---|---|
| empirical formula | $C_{27}H_{34}DyP$ | $C_{70}H_{83}Dy_3P_3$ | $Dy_3P_3C_{99}H_{132}O_9Li_3$ | $C_{27}H_{34}YP$ | $C_{70}H_{83}Y_3P_3$ | $Y_3P_3C_{99}H_{147}O_9Li_3$ |
| formula weight | 552.01 | 1504.77 | 2067.27 | 478.42 | 1284.00 | 1861.62 |
| temperature / K | 100(2) | 150(1) | 150(1) | 100(2) | 150(2) | 150(1) |
| crystal system | monoclinic | monoclinic | monoclinic | monoclinic | monoclinic | monoclinic |
| space group | $P2_1/n$ | $Cc$ | $P2_1/c$ | $P2_1/n$ | $P2_1/c$ | $P2_1/c$ |
| $a$ / Å | 8.1970(5) | 14.8953(6) | 22.3210(5) | 8.1790(6) | 11.6328(4) | 22.3184(10) |
| $b$ / Å | 24.7447(18) | 18.6307(8) | 15.7702(3) | 24.6788(18) | 25.0914(10) | 15.7523(10) |
| $c$ / Å | 11.5021(10) | 23.6059(9) | 27.9921(7) | 11.5031(10) | 21.5705(7) | 27.9702(14) |
| $\alpha$ / ° | 90 | 90 | 90 | 90 | 90 | 90 |
| $\beta$ / ° | 94.741(7) | 103.260(4) | 95.319(2) | 94.707(6) | 91.002(3) | 91.358(4) |
| $\gamma$ / ° | 90 | 90 | 90 | 90 | 90 | 90 |
| volume / Å$^3$ | 2325.0(3) | 6376.3(5) | 9811.0(4) | 2314.0(3) | 6295.1(4) | 9790.4(9) |
| $Z$ | 4 | 4 | 4 | 4 | 4 | 4 |
| $\rho_{calc}$ / mg mm$^{-3}$ | 1.577 | 1.568 | 1.400 | 1.373 | 1.355 | 1.263 |
| crystal size / mm$^3$ | 0.5 × 0.3 × 0.2 | 0.4 × 0.2 × 0.15 | 0.5 × 0.3 × 0.2 | 0.2 × 0.1 × 0.05 | 0.1 × 0.05 × 0.02 | 0.5 × 0.1 × 0.02 |
| 2$\theta$ range/° | 5.88-52.744 | 6.888-52.726 | 6.288-50.7 | 5.89-52.742 | 7.46-52.746 | 6.512-50.7 |
| reflections collected | 9055 | 23340 | 29590 | 9217 | 37554 | 37632 |
| independent reflections | 4745 | 9579 | 17805 | 4724 | 12814 | 17853 |
| $R$(int) | 0.0419 | 0.0737 | 0.0331 | 0.0645 | 0.0456 | 0.0797 |
| data/restraints/parameters | 4745/68/316 | 9579/131/701 | 17805/18/1107 | 4724/0/286 | 12814/178/729 | 17853/333/1275 |
| goodness-of-fit on $F^2$ | 1.039 | 1.064 | 1.037 | 1.028 | 1.039 | 0.992 |
| final $R$ indexes [I≥2σ(I)] | $R_1$ = 0.0382<br>$wR_2$ = 0.0841 | $R_1$ = 0.0570<br>$wR_2$ = 0.1221 | $R_1$ = 0.0429<br>$wR_2$ = 0.0917 | $R_1$ = 0.0529<br>$wR_2$ = 0.1082 | $R_1$ = 0.0570<br>$wR_2$ = 0.1423 | $R_1$ = 0.0607<br>$wR_2$ = 0.0881 |
| final $R$ indexes [all data] | $R_1$ = 0.0487<br>$wR_2$ = 0.0932 | $R_1$ = 0.0660<br>$wR_2$ = 0.1307 | $R_1$ = 0.0589<br>$wR_2$ = 0.1011 | $R_1$ = 0.0971<br>$wR_2$ = 0.1415 | $R_1$ = 0.0937<br>$wR_2$ = 0.1604 | $R_1$ = 0.1366<br>$wR_2$ = 0.1080 |
| largest diff. peak, hole /e.A$^{-3}$ | 1.81, –1.83 | 3.39, –1.05 | 1.44, –1.12 | 0.76, –0.91 | 0.83, –2.03 | 0.41, –0.41 |

**Supplementary Table 2.** Selected bond lengths (Å) and angles (°) for **1-Dy**, **2-Dy** and **3-Dy**

| | **1-Dy** | **2-Dy** | **3-Dy** |
|---|---|---|---|
| Dy–P | 3.009(1) | 2.926(6)-2.951(6) | 2.7850(15)-2.8249(15) |
| Dy–C | 2.676(7)-2.744(6) | 2.60(2)-2.72(1) | 2.625(6)-2.762(6) |
| Dy–$Cp_{cent}$ | 2.420(5)-2.443(5) | 2.345(8)-2.369(7) | 2.385(3)-2.441(3) |
| Li–P | | | 2.472(9)-2.557(9) |
| P-Dy-P | | 89.23(18)-98.49(18) | 90.95(4)-93.99(4) |
| $Cp_{cent}$-Dy-$Cp_{cent}$ | 117.73(10)-118.56(10) | 126.0(3)-126.4(3) | 121.23(10)-123.96(10) |
| Dy-P-Dy | | 128.65(17)-134.35(18) | 131.08(5)-134.99(5) |
| P-Li-P | | | 107.0(3)-109.6(4) |
| Dy-P-Li | | | 76.9(2)-80.5(2) |

**Supplementary Table 3.** Selected bond lengths (Å) and angles (°) for **1-Y**, **2-Y** and **3-Y**

| | **1-Y** | **2-Y** | **3-Y** |
|---|---|---|---|
| Y–P | 3.010(1) | 2.923(2)-2.954(2) | 2.7869(12)-2.8269(13) |
| Y–C | 2.661(6)-2.749(5) | 2.614(7)-2.67(1) | 2.633(4)-2.760(6) |
| Y–$Cp_{cent}$ | 2.416(5)-2.444(5) | 2.337(7)-2.362(7) | 2.379(2)-2.430(2) |
| Li–P | | | 2.468(8)-2.546(8) |
| P-Y-P | | 86.33(5)-91.23(5) | 91.03(4)-94.06(4) |
| Y-P-Y | | 135.48(7)-137.74(6) | 131.29(5)-135.27(5) |
| P-Li-P | | | 106.8(3)-109.4(3) |
| Y-P-Li | | | 77.32(18)-79.99(19) |

**Supplementary Table 4.** Energies of the low-lying Kramers doublets for **1-Dy**.

| Kramers Doublet | Energy / $cm^{-1}$ |
|---|---|
| 1 | 0.000 |
| | 0.000 |
| 2 | 45.212 |
| | 45.212 |
| 3 | 98.749 |
| | 98.749 |
| 4 | 287.170 |
| | 287.170 |
| 5 | 339.555 |
| | 339.555 |
| 6 | 391.739 |
| | 391.739 |
| 7 | 452.533 |
| | 452.533 |
| 8 | 583.953 |
| | 583.953 |

**Supplementary Table 5.** *g*-Tensors for the low-lying Kramers doublets for $Dy^{3+}$ in **1-Dy**.

| Kramers doublet | | Dy1 |
|---|---|---|
| 1 | $g_x$ | 0.88625 |
| | $g_y$ | 5.41752 |
| | $g_z$ | 15.01699 |
| 2 | $g_x$ | 2.59868 |
| | $g_y$ | 3.35940 |
| | $g_z$ | 6.35830 |
| 3 | $g_x$ | 10.17715 |
| | $g_y$ | 6.96903 |
| | $g_z$ | 2.52102 |
| 4 | $g_x$ | 5.20707 |
| | $g_y$ | 7.16596 |
| | $g_z$ | 9.70857 |
| 5 | $g_x$ | 1.07105 |
| | $g_y$ | 1.56443 |
| | $g_z$ | 10.88776 |
| 6 | $g_x$ | 1.26191 |
| | $g_y$ | 1.89979 |
| | $g_z$ | 13.67944 |
| 7 | $g_x$ | 1.71010 |
| | $g_y$ | 1.79953 |
| | $g_z$ | 16.47939 |
| 8 | $g_x$ | 0.04281 |
| | $g_y$ | 0.04719 |
| | $g_z$ | 19.67566 |

**Supplementary Table 6.** Energies of the low-lying Kramers doublets for **2-Dy**.

| Kramers doublet | Energy / $cm^{-1}$ | | |
|---|---|---|---|
| | Dy1 | Dy2 | Dy3 |
| 1 | 0.000 | 0.000 | 0.000 |
| | 0.000 | 0.000 | 0.000 |
| 2 | 126.738 | 134.260 | 135.048 |
| | 126.738 | 134.260 | 135.048 |
| 3 | 277.317 | 296.823 | 297.883 |
| | 277.317 | 296.823 | 297.883 |
| 4 | 345.800 | 320.995 | 334.413 |
| | 345.800 | 320.995 | 334.413 |
| 5 | 362.707 | 388.786 | 381.074 |
| | 362.707 | 388.786 | 381.074 |
| 6 | 402.858 | 431.024 | 419.049 |
| | 402.858 | 431.024 | 419.049 |
| 7 | 433.617 | 499.247 | 478.016 |
| | 433.617 | 499.247 | 478.016 |
| 8 | 551.778 | 675.677 | 637.826 |
| | 551.778 | 675.677 | 637.826 |

**Supplementary Table 7.** *g*-Tensors for the low-lying Kramers doublets for $Dy^{3+}$ in **2-Dy**.

| Kramers doublet | | Dy1 | Dy2 | Dy3 |
|---|---|---|---|---|
| 1 | $g_x$ | 0.00033 | 0.00196 | 0.00029 |
| | $g_y$ | 0.00047 | 0.00367 | 0.00050 |
| | $g_z$ | 19.43021 | 19.30007 | 19.45874 |
| 2 | $g_x$ | 0.00115 | 0.02129 | 0.00306 |
| | $g_y$ | 0.00155 | 0.02269 | 0.00324 |
| | $g_z$ | 17.04631 | 16.85113 | 16.96575 |
| 3 | $g_x$ | 0.02891 | 1.06941 | 0.14877 |
| | $g_y$ | 0.03023 | 2.62004 | 0.23083 |
| | $g_z$ | 14.88347 | 13.21101 | 14.80977 |
| 4 | $g_x$ | 10.05515 | 1.22690 | 0.11165 |
| | $g_y$ | 5.86141 | 1.91332 | 0.68495 |
| | $g_z$ | 1.63782 | 14.44525 | 19.14349 |
| 5 | $g_x$ | 10.10938 | 3.31114 | 2.64013 |
| | $g_y$ | 5.26252 | 4.49971 | 3.31519 |
| | $g_z$ | 0.20865 | 9.74614 | 10.71650 |
| 6 | $g_x$ | 3.47925 | 3.45545 | 3.74371 |
| | $g_y$ | 5.70108 | 5.58090 | 6.68520 |
| | $g_z$ | 9.91449 | 11.17103 | 10.54301 |
| 7 | $g_x$ | 1.19063 | 0.62235 | 0.55815 |
| | $g_y$ | 2.77104 | 1.04659 | 1.13718 |
| | $g_z$ | 14.49222 | 16.60486 | 16.44954 |

**Supplementary Table 8.** Energies of the low-lying Kramers doublets for **3-Dy**.

| Kramers doublet | Energy / $cm^{-1}$ | | |
|---|---|---|---|
| | Dy1 | Dy2 | Dy3 |
| 1 | 0.000 | 0.000 | 0.000 |
| | 0.000 | 0.000 | 0.000 |
| 2 | 58.247 | 64.365 | 95.241 |
| | 58.247 | 64.365 | 95.241 |
| 3 | 78.371 | 78.250 | 104.321 |
| | 78.371 | 78.250 | 104.321 |
| 4 | 103.435 | 97.406 | 120.807 |
| | 103.435 | 97.406 | 120.807 |
| 5 | 122.389 | 135.092 | 140.892 |
| | 122.389 | 135.092 | 140.892 |
| 6 | 146.971 | 145.203 | 166.755 |
| | 146.971 | 145.203 | 166.755 |
| 7 | 168.885 | 168.820 | 193.711 |
| | 168.885 | 168.820 | 193.711 |
| 8 | 223.029 | 263.709 | 286.325 |
| | 223.029 | 263.709 | 286.325 |

**Supplementary Table 9.** *g*-Tensors for the low-lying Kramers doublets for $Dy^{3+}$ in **3-Dy**.

| Kramers doublet | | Dy1 | Dy2 | Dy3 |
|---|---|---|---|---|
| 1 | $g_x$ | 0.00423 | 0.01492 | 0.00503 |
| | $g_y$ | 0.00837 | 0.02902 | 0.00806 |
| | $g_z$ | 19.49151 | 19.24095 | 19.68294 |
| 2 | $g_x$ | 0.86405 | 0.16320 | 1.22502 |
| | $g_y$ | 1.09542 | 0.26337 | 2.56564 |
| | $g_z$ | 17.50331 | 18.59501 | 14.52369 |
| 3 | $g_x$ | 0.21328 | 1.51492 | 0.13761 |
| | $g_y$ | 0.97434 | 4.63478 | 1.15670 |
| | $g_z$ | 17.59941 | 13.90572 | 16.39110 |
| 4 | $g_x$ | 2.22590 | 8.01559 | 2.50449 |
| | $g_y$ | 3.49025 | 5.43461 | 3.41616 |
| | $g_z$ | 12.14247 | 0.96668 | 11.47954 |
| 5 | $g_x$ | 1.68286 | 1.14957 | 0.66293 |
| | $g_y$ | 3.40168 | 2.77558 | 1.51748 |
| | $g_z$ | 14.01526 | 10.03090 | 14.19471 |
| 6 | $g_x$ | 0.88140 | 0.70816 | 0.52837 |
| | $g_y$ | 2.46254 | 3.34131 | 2.96868 |
| | $g_z$ | 12.83301 | 14.26587 | 12.89100 |
| 7 | $g_x$ | 0.51028 | 2.26081 | 1.64233 |
| | $g_y$ | 2.40652 | 2.68398 | 2.57990 |
| | $g_z$ | 16.19778 | 14.97747 | 16.47459 |
| 8 | $g_x$ | 0.45265 | 0.13082 | 0.20210 |
| | $g_y$ | 1.49304 | 0.24894 | 0.51674 |
| | $g_z$ | 17.74837 | 18.92904 | 18.72388 |

**Supplementary Table 10.** Exchange coupling and dipolar coupling parameters and the spectrum of exchange Kramers doublets in **2-Dy** and **3-Dy** ($cm^{-1}$).

| Interaction | | **2-Dy** | **3-Dy** |
|---|---|---|---|
| dipolar* | Dy1-Dy2 | –1.116 | –1.210 |
| | Dy2- Dy3 | –1.202 | –1.232 |
| | Dy3- Dy1 | –1.110 | –1.221 |
| exchange | Dy1- Dy2 | –3.014 | –1.492 |
| | Dy2- Dy3 | –2.878 | –1.495 |
| | Dy3- Dy1 | –2.991 | –1.528 |
| Exchange spectrum | 1 | 0.0000 | 0.0000 |
| | 2 | 0.0035 | 0.0261 |
| | 3 | 0.0198 | 0.0286 |
| | 4 | 3.8459 | 2.6240 |

* Only the term of the dipolar interaction is shown here. In the POLY_ANISO calculation, all terms were included.